Durability of Hydrostab; a field investigation and prognosis

Commissioned by BKB Waste-Management bv

Durability of Hydrostab; a field investigation and prognosis

D. Boels
J. Bril (GeQuiMa)
E. Hummelink
O. Boersma

Alterra-report 1218

Alterra, Wageningen, 2005

ABSTRACT

Boels, D., J. Bril (GeQuiMa), E. Hummelink and O. Boersma 2005. *Durability of Hydrostab; a field investigation and prognosis*. Wageningen, Alterra, Alterra-report 1218. 54 pp.; 10 fig.; 6 tab.; 36 ref.

Eight years after installation on a test site, the enclosing properties of Hydrostab are undiminished and satisfy the requirements of the Dutch Decree on Soil Protection for Disposal to Landfill ("Stortbesluit" 1993). Also no change was found in the moisture content. Analysis of the processes and components that determine the characteristics of Hydrostab shows that C-S-H- and C-A-H-gels form from fly ash which subsequently fall apart and produce silica gels. In this process the capillary pore space initially decreases. Only after transformation of all C-S-H and C-A-H into silica-gel the amount of gel in the soil pores decreases slowly, producing the final end product quartz. In this process the capillary pore space increases. When the value of the capillary pore space increases above 0.18, the sealing properties of Hydrostab decrease. This moment in time can therefore be marked as the end of the functional lifetime of the Hydrostab. Dependent on model parameterization this moment is 180 - 500 years in the future.

Keywords: "Stortbesluit", permeability, moisture, silica-gel, capillary pore space, durability

ISSN 1566-7197

This report can be ordered by paying € 25,- to bank account number 36 70 54 612 by name of Alterra Wageningen, IBAN number NL 83 RABO 036 70 54 612, Swift number RABO2u nl. Please refer to Alterra-report 1218. This amount is including tax (where applicable) and handling costs.

P.O. Box 47; 6700 AA Wageningen; The Netherlands
Phone: + 31 317 474700; fax: +31 317 419000; e-mail: info.alterra@wur.nl

Contents

Preface

This research has been commissioned by BKB Reststoffenmanagement, Dalfsen. Aim of the study is to generate a substantiated prognosis of the functional life expectancy (durability) of Hydrostab and when possible to show that the estimated life expectancy as used by the IPO after-care systematics (which is set at 50 years) might need some adjustment.

The field investigations were carried out on a plot on the "Boeldershoek" waste disposal site, Hengelo, which has been created in 1994. We are grateful to the owners of this waste disposal site for their cooperation to this study.

The analysis of the chemical processes and the geochemical modelling were performed in cooperation with Legiolabs, Leiden and GeQuiMa, Lisbon, Portugal (drs. J. Bril). The chemical analysis of the pore water in the different layers have been carried out at the laboratory of the department of Soil Quality of Wageningen Agricultural University.

Abstract and Conclusions

Hydrostab is a mixture of residues to which soluble alkalisilicates ("waterglass") have been added. It is used as a mineral barrier in the top sealing of waste disposal sites.

Research upto now has indicated that Hydrostab is durable and possibly "everlasting". However, since the processes that influence the life expectancy were not inventarized in detail and also not quantitatively understood, the present IPO after-care systematics set the life expectancy of Hydrostab to 50 years.

The aim of the field, laboratory and desk research which is described in this report is to illuminate the processes that determine the chemical stability of Hydrostab and to make an educated prognosis of the life expectancy.

The functionality of Hydrostab as a top sealing has been re-investigated at the test plot of the waste disposal site "Boeldershoek", Hengelo, eight years after the construction of the plot. The investigation showed that the bulk density has increased since 1996, but the moisture content of the Hydrostab layer did not change. Although this had been expected, it is remarkable since the Hydrostab was applied as a single layer, without foil coverage as is used in practical applications elsewhere, and therefore was potentially subjected to drying and wetting cycles.
From the analysis of the leaching of conservative substances (chloride and sulphur) is derived that the actual waterflow through the Hydrostab on the middle and at the foot of the slope of the test plot is less than 1 mm per year, and at the top is about 1 mm per year. This extremely low infiltration probably can be attributed to a well functioning Hydrostab layer combined with a fast drainage of surface infiltration through the sandy cover. Measurements of the actual conductivity of Hydrostab confirm the low permeability and show that the Hydrostab layer at present confirms easily to the qualification demands of the Dutch Decree on Soil Protection for Disposal to Landfill ("Stortbesluit").

Inventarization of the processes responsible for the sealing functionality of the Hydrostab show, that due to interactions between components of the Hydrostab different types of silicate-containing gels are formed. The gel that initially formes from the fly ash (one of the components of the Hydrostab), C-S-H-gel (Calcium-Silicate-Hydrate), is not stable and slowly disintegrates., thereby producing silica-gel. In the first years after the construction the amount of silica-gel, which partly was formed from the waterglass, increases and therefore the capillary porespace decreases, thereby decreasing the permeability of the Hydrostab layer. Once all the C-S-H-gel has disappeared, the amount of silica-gel will slowly decrease. The silica-gel will produce another, (gel ?) substance, Opal-CT (Cristobalite - Tridymite). This in its turn will in time produce cristalline Quartz. In the course of these transformations the gel-volume decreases and therefore the capillary pore space increases.

The permeability of the Hydrostab is determined by the capillary pore space. As long as the capillary pore space is less than 0.18, all continuous pores are blocked and mass transport can only be achieved by diffusion through the gel-water phase. When the capillary pore space rises above 0.18, continuous pores appear and the sealing function of the Hydrostab deminishes.

This moment has been calculated using physical and physico-chemical modelling. Assuming very conservative ("worst case") approximations of reaction rates the life expectancy of the Hydrostab has been calculated as at least 180 years. More realistic and recently evaluated reaction rates give life expectancies of 500 years or more.

1 Introduction

1.1 Problem definition

Hydrostab is a mixture of residues which have been bound together by the addition of waterglass (soluble sodiumsilicate). It is used as a mineral sealing in the top capping (roofing) of waste disposal sites.
Research has shown that Hydrostab is durable, possibly permanent. However, in the present-day IPO after-care systematics the life expectancy of Hydrostab is put at 50 years, whereas a mixture of sand-bentonite and Trisoplast (an organic polymere) is put at 75 years. This difference has been made since the processes which control the permeability of Hydrostab were not sufficiently understood.
The current study draws up an inventory of the processes governing the permeability of Hydrostab, and provides a prognosis for the life expectancy. In this report "permeability" and "hydraulic conductivity" are often used interchangeably. Technically speaking, a soil has an "intrinsic" permeability that is a function of the media properties only (units of length-squared), whereas hydraulic conductivity is a function of both media and fluid properties (units of length per time). If "permeability" is reported in length per time units, it is the same as hydraulic conductivity.

1.2 Background

Hydrostab is produced from residues such as: fly ash, sewage sludge, paper mill sludge, screening sand, green sand and other casting sands, (Boels & Beuving, 1996), onto which waterglass is added. Waterglass is a collective noun for water soluble alkali-silicates (Na- or K-) which are produced by melting together at 1500 ^{o}C quartz (SiO_2) and alkali-carbonate. Chemically the alkali-silicates can be classified by the ratio SiO_2/MeO, where Me can be Na_2 or K_2 (Belouschek & Novotny, 1989; Boels et al., 1993). Waterglass is commercially available as a liquid or as a powder.
Together with the colloids of the sewage sludge the waterglass forms a silicate sol-gel that fills the available pore space and encloses virtually all capillary pores. The permeability of the mixture is therefore greatly reduced (Grattoni, et al, 2001). Hydrostab has an extremely low hydraulic conductivity ($< 4.10^{-10}$ m/s). Hydrostab is used in layers of about 0.5 m thickness in the top enclosing constructions of waste disposal sites. On top of the Hydrostab layer often a foil is applied. To meet the criteria of the Dutch Decree on Soil Protection for Disposal to Landfill ("Stortbesluit") the hydraulic conductivity of Hydrostab in standard conditions (1 m water column with free drainage at the bottom) must be lower than 4×10^{-10} m/s.
Because of the combined sealing (mineral + foil) theoretically no percolation of rainwater is possible. However, even with well constructed foil layers little cracks and splits can appear, and therefore the mineral layer functions as a second barrier. Below the Hydrostab layer is a support layer which separates the Hydrostab from the waste

depot. Diffusive processes will transport substances between the Hydrostab layer and the support layer and possibly also the waste.
The main body of waste is not inert and can in time show some setting. To maintain its enclosing functionality the Hydrostab layer has to be able to deform plastically as well. Deformation tests have shown that Hydrostab behaves like a plastic material and with a uniform stress of 10 % keeps its initial (low) permeability.

Dehydration, a process that could destroy the sol-gel structure, has been investigated in the field study. The measurements of the water pressure in the Hydrostab enclosing layer only show marginal variations in time.
Figure 1 shows the development of the water pressure in the Hydrostab layer at the RAZOB waste disposal site (Nuenen, the Netherlands). The water pressure found is about -100 cm water column (~ -100 mBar, pF=2). This pressure is related to the moisture content and for each mineral material a unique relation exists between moisture content and water pressure. A water pressure of 0 cm shows a water saturated material, whereas an air-dry material is characterized by a pressure of about -100,000 mBar (pF=5). The loss of moisture between a tension of 0 and -100 cm H_2O is in materials comparable to Hydrostab about 2%. The variations found in moisture content of the Hydrostab layer within a year are thus less than +/- 0.8%. This means the moisture content of the Hydrostab is almost constant, with only minor variations.

Based on this investigation and model calculations it can be shown that dehydration due to cyclic variations of temperature and temperature gradients in constructions with foil is not probable and that moisture changes are negligible.

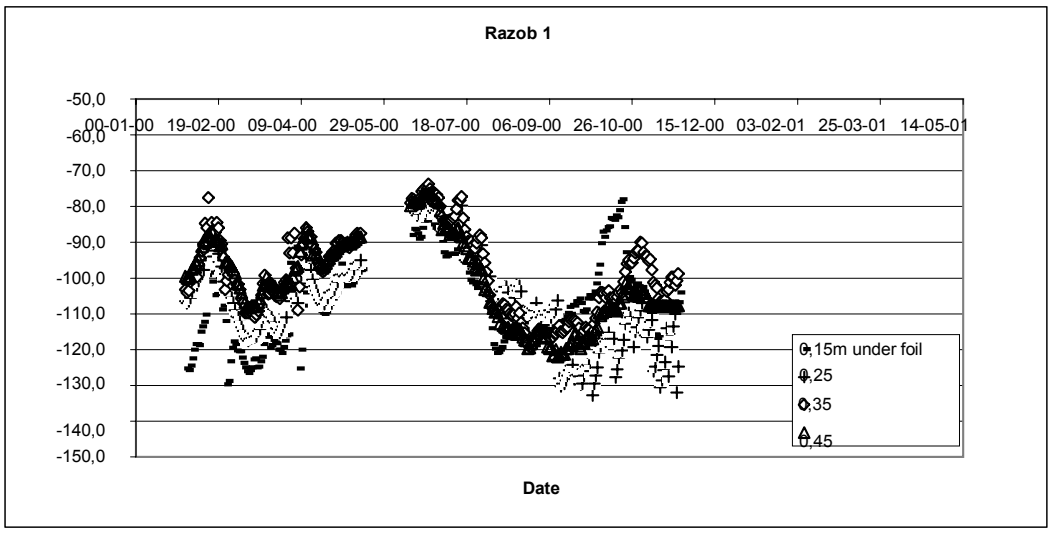

Figure 1 Changes in water tension of a Hydrostab-layer on top of the RAZOB waste disposal site

1.3 Project goals

The aim of this project is twofold. First aim is to establish the existence of processes capable of changing the stability of the sol-gel.
Second, an investigation at an old test-site has to show if and how far the original low permeability has been maintained, and if leaching has occurred.

The test-site comprises an experiment where Hydrostab is the only enclosing layer (no foil was applied) and therefore the Hydrostab has possibly been subject to cyclic drying and wetting.

2 Materials and Methods

2.1 Sampling and sample selection

The test site "Boeldershoek" at Hengelo (the Netherlands) was constructed in connection with the Tender-procedure "T2000 Immobilization 1993", by a consortium of the following companies and governmental organizations: Verhoeve Milieu (Hummelo), Samenwerkingsverband Twente (Hengelo), AKZO-PQ Silica (Amersfoort) and the ministry of the environment (VROM, Den Haag)
(BKB, 1995a, b; Siedek en Kügler, 1995). NOVEM (Dutch governmental agency for energy and the environment) partly coordinated and financed the research. BKB-Reststoffen Management instigated and coordinated the project.

In 2004, on three different locations (at the foot, in the middle and at the top of a slope) on this test site, profile pits were dug to enable a description of the profile structure, to visually inspect the Hydrostab layer for the appearance of concretions, and for the sampling to determine moisture content, bulk density and hydraulic conductivity. Also samples were taken to enable chemical analysis of the pore water in the layers: 0.25 m above the Hydrostab layer, the upper and lower part of the Hydrostab layer, and the layers 0 – 0.25, 0.25 – 0.50; 0.50 – 0.75 and 0.75 – 1.00 m below the Hydrostab layer (insofar this didn't fall in the waste). Pictures were taken.

Sampling:

1. Cover layer: For each pit two mixed samples
2. Pore water analysis: pH, EC, Cl, Ca, Mg, Na, K, Fe. Al, P, S, TOC, DOC
3. HYDROSTAB: For each pit and for each layer of 0.25 m: two mixed samples
4. Pore water analysis: pH, EC, Cl, Ca, Mg, Na, K, Fe. Al, P, S, Si, TOC, DOC
5. HYDROSTAB: For each pit 3 samples for hydraulic conductivity, and 4 samples for bulk density determination.
6. Support Layer: 2 mixed samples from the first 0.25 m below the Hydrostab for the analysis of pore water: pH, EC, Cl, Ca, Mg, Na, K, Fe. Al, P, S, Si, TOC, DOC;
7. Support Layer: For each pit for all other layers: 2 mixed samples for the analysis of pore water: pH, EC and Cl.

2.2 Hydraulic Conductivity Measurements

Samples were taken from the Hydrostab layers for the laboratory measurement of the hydraulic conductivity. Columns were prepared and adjusted to the required diameter. The prepared columns were placed in a sampling ring. The space between the Hydrostab columns and the sampling ring (about 1 cm) was filled with dry bentonite powder. The columns were used to measure the hydraulic conductivity

according to the"falling head" method. With this method the sample is enclosed in a rigid cylinder between two filters. Liquid is supplied from a gauge tube with a graduation scale
Upward flow has been chosen to prevent air inclusions during the saturation of the sample. Discharge of liquid is on the top of the sample at a fixed hight. During the measurement the level of the liquid in the gauge tube decreases. The volume that flows through the sample is proportional to the decrease. The level of the liquid is also a measure of the pressure drop over the sample. The hydraulic conductivity is determined from the difference in pressure head at two consecutive moments in time according to:

$$K_{sat} = -(1/\Delta T)\,(a_{Tube}/A_{sample})\,\mathbf{ln}\,\{h(T+\Delta T)/h(T)\}$$

Where

Ksat	permeability (m/s)
ΔT	time between two measurements (s)
aTube	surface area of gauge tube (0.0000283 m2)
Asample	Surface area of the sample (0.00785 m2)
h(T)	level of liquid in gauge tube relative to outflow at time T
ln {…}	natural logarithm

Measurements are performed until the permeability is constant .

2.3 Bulk Density

While installing the measurement apparatus for the Hydraulic Conductivity samples of 100 cm^3 were taken for the determination of bulk density. The bulk density was measured by drying the samples for a period of 24 hours at 105 ^oC. Dividing the weight of the dried sample (in kg) by the initial volume (in m^3) gives the bulk density in kg/m^3

2.4 Chemical analysis

To determine the chemical composition of the pore water in the samples, the samples were first incubated with water (25 % of the dry weight) and after incubation centrifuged. In the liquid the pH, Ec (electrical conductivity) and Cl were measured and after a 5-10 fold dilution the macro-parameters Ca, Mg Na, K, Fe, Al, P, S, TOC and DOC were determined using ICP (Thermo Jarrell Ash).

2.5 Leaching of Hydrostab;

Hydrostab contains dissolved, conservative substances like chloride and sulphate that potentially can leach. The presence and concentration of these substances in the soil layer under the Hydrostab has been investigated. From the concentrations found the leaching from the Hydrostab layer can de deduced. Also the total amount of percolation water from the construction until the moment of investigation can be assessed.

2.6 Evaluation Durability Hydrostab

2.6.1 Methodology

Theoretically, the functionality of Hydrostab can diminish by the following processes:

1. Fracture formation due to strain developing by irregular setting of the waste depot.
2. Increase of the effective porosity by moisture loss (dehydration) which affects irreversibly the gel structure ;
3. Disappearance of gel structure by chemical reactions that transform silica-gel into cristalline quartz, increasing the effective porosity.

It has been shown that the first two processes do not cause a decrease of the functionality of Hydrostab in the conditions which are prevalent at Dutch disposal sites.

However, the third process has not been invalidated. Immediately after the application of Hydrostab a number of reactions start. First a silica-sol is formed from the waterglass solution. This sol reacts, influenced by cations which are present, oxides of iron and (phenolic and alcoholic groups of) the organic matter, to form a diverse array of different types of silica-gels with a high pore-volume. Because of the gel formation the capillary pore space reduces to a level where no continuous pathways are present anymore, thereby effectively closing the Hydrostab for transport of liquids. The silica-gels are meta-stable phases. They will, dependent on environmental parameters, transform into quartz and in the process of this transformation loose their structure. The transformation of silica-gel into quartz passes through the formation of Opal-CT (CT = Cristoballite-Tridymite) as an itermediate and is a slow process.

The methodology for the approximation of the life expectancy of Hydrostab consists of the calculation of the rate with which the silica-gels are transformed into quartz. In the course of this transformation the effective (capillary) porosity increases, which has repercussions on the hydraulic conductivity. This research also presents a limiting value for the capillary porosity, enabling the establishment of a moment in time when the Hydrostab will not meet the criteria of the "Stortbesluit" any more.

2.6.2 Geochemical modelling

A geochemical model has been developed to calculate the course of the transformation of silica-gel into quartz. A part of this model comprises the speciation of silica in the pore water. To calculate and calibrate the speciation of silica in the pore water the measured composition of the macrochemistry of the pore waters in the Hydrostab is used.

Assuming the exchange of dissolved substances in the pore water of the Hydrostab layer, the sandy top layer above the Hydrostab and the support layer beneath by diffusion, the change in pore water chemistry has been calculated. The pore water composition influences the silica-gel stability. The functionality of the Hydrostab layer remains intact as long as the silica-gel structure is not changed too much. It is assumed here that the Hydrostab does not dry out, as was made clear in the research presented before.

3 Field Investigation Results

3.1 Profile Description

In three locations, on the foot, in the middle and at the top of the slope of the test site, profile pits have been dug. Tables 1 to 3 give a description of the profiles. Pictures of the pits are presented in annex 1 and 2.

Table 1 Description of profile 1, foot of the slope

Layer (cm – mv)	Description	Remark
0 – 45	Humic sand, mixed with humus-free sand	
45 – 55	Hydrostab upper layer	
55 – 55	Geo-foil	
55 – 75	Hydrostab lower layer	
75 – 110	Mixture sand (~140 μm) + loam (~10%)	sample in layer 85 - 110
110 – 135	Mixture sand (~140 μm) + loam (~10%)	sample
135 – 165	Mixture sand and loam	sample

Table 2 Description of profile 2, middle of the slope

Layer (cm – mv)	Description	Remark
0 – 35	Coarse sand (low humics)	
35 – 55	Hydrostab, upper layer	
55 – 55	Geo-foil	
55 – 65	Hydrostab, lower layer	
65 – 80	Black soil, ~10% organic matter	
80 – 100	Brown sand + some yellow sand	Sample
100 – 130	Yellow sand	Sample
130 – 160	Brown and yellow sand	Sample
160 – 180	Gray sand	Sample

Table 3 Description of profile 3, top of the slope

Layer (cm – mv)	Description	Remark
0 – 68	Pure white sand	Rooting depth < 20 cm. Sand is saturated near the Hydrostab.
68 – 98	Hydrostab	
98 – 100	Clay layer	
100 – 120	Sand	Sample
120 – 140	Sand	Sample
140 – 165	Sand	Sample
165 – 195	Sand	Sample

The rooting depth of the vegetation is limited and does not reach the Hydrostab layer.
The top layers and the supporting layers are mixed. The Hydrostab layer has no gradation characteristics. On the top of the slope the water table (the saturation level) was on top of the Hydrostab layer. Sand and water flowed into the profile pit.

3.2 Bulk density and moisture content.

Table 4 gives the measured bulk density and moisture content of the Hydrostab layer.

Table 4 Moisture content and bulk density of Hydrostab in 2004, compared to measurements of 1996

Location	Profile	layer	Moisture (% dry weight)		Bulk Density (kg/m³)	
			1996	2004	1996	2004
Foot	1	upper	39.8 – 41.9	40.2	1057 - 1078	1202
Foot	1	upper		51.1		1069
Foot	1	lower		40.1		1194
Foot	1	lower		42.9		1137
Middle	2	upper	29.8 – 38.4	37.3	1235	1240
Middle	2	upper		35.4		1282
Middle	2	lower		22.8		1346
Middle	2	lower		27.2		1335
Top	3	upper	36.7 – 43.5	32.9	1129	1277
Top	3	upper		34.0		1291
Top	3	lower		36.7		1250
Top	3	lower		34.9		1274

This table shows that in 2004 on average the moisture content of Hydrostab at the top of the slope seems to be lower than measured in 1996. The middle of the slope shows no change, whereas at the foot of the slope the moisture content seems to be higher in 2004 than in 1996. However, the amount of moisture (kg water/m^3 soil) did not change in the top and middle of the slope, but increased somewhat in the foot. The conclusion is that in about 8 years no significant change in moisture content did occur.
The bulk density has increased somewhat which indicates some consolidation.

3.3 Permeability

Table 5 gives the results of the measurements of hydraulic conductivity. Some measurements did not produce reliable values because rubble caused a side-effect that with the used method cannot be measured separately. In some samples gas development was observed, which made the test liquid flow back instead of through the samples. These measurements have been excluded.

Table 5 shows that the variability of the hydraulic conductivity was relatively high in 1996: from 0.7 – 6.4 x 10^{-10} (averageing 2.8 x 10^{-10}) m/s. In 2004 the measurements varied between 1.08 – 3.73 x 10^{-10} (averageing 2.1 x 10^{-10}) m/s. Based on the averages and the distributions it can be concluded that the hydraulic conductivity did not change during the last 8 years. The measured values are lower than 3.9 x 10^{-10} m/s, the value required by law ("Stortbesluit") for a layer of 0.5 m.

Table 5: Results of the hydraulic conductivity measurements

location	Profile	layer	Bulk Density (kg/m³)	Permeability (x 10^{-10} m/s)	
			2004	1996	2004
Foot	1	upper	994	1.4 - 3.0	disturbed
Foot	1	upper			
Foot	1	lower	1144		
2.22 Foot	1	lower	1124		
1.24 Middle	2	upper	1196	0.7 -	
1.4 3.40 Middle	2	upper			
Middle	2	lower	1259		gas
Middle	2	lower	1278		1.08
Top	3	upper	1272	3.9 - 6.4	1.74
Top	3	upper			
Top	3	lower	1185		3.73
Top	3	lower	1199		1.47

Disturbed: rubble and gravel give unreliable results

Gas: Gas development makes measurement impossible

3.4 Estimation of actual seepage

The "real" seepage through the enclosing layer can also be estimated from a reconstruction of the leaching of dissolved substances from the Hydrostab layer. It is assumed that the moisture content and the flux (the convective flow of water) of all layers is constant, and average throughout time. It is also assumed that all layers are perfectly mixed and that ad/desorption and precipitation/dissolution does not play any role. Therefore the calculations have been performed for chloride and dissolved sulphur (which is mainly sulphate). The calculation scheme used is:

$$c_t = (c_0 - c_i)\, e^{(1/T)}$$

Where:

c_t	concentration on time t
c_0	concentration on time t=0
c_i	concentration of the incoming flux
T	residence time {= f / (θd) } (days)
f	flux (m/day)
d	layer thickness (m)
θ	moisture content ($m^3.m^{-3}$)

The average concentration of the flux that leaves the segment and enters the receiving segment as c_i is:

$$c_{Av} = c_i + (c_0 - c_i)\,(T/t)\,\{1 - e^{(t/T)}\}$$

The calculation scheme divides the profile in a number of small layers. For each layer the moisture content and the thickness are input. The initial values of the concentration are estimated, and the concentration in the upper boundary is supplied. Then for an 8 year period the changes in concentration are calculated, and compared to the measured values (averaged for layers of 0.25 m). The flux and the initially estimated concentration distribution are adjusted until the calculated concentrations after 8 years (almost) coincide with the measured values. Then a reasonable estimate of the average flux has been obtained (see figure 2).

Both Chloride and Sulphur leaching calculations show that the water flux in the foot and in the middle of the slope is less than 1 mm/year. The top of the slope gives a water flux of 1 mm/year. This very small infiltration can probably be attributed to fast discharge through the covering sandy top layer, and a complete closure of all capillary pores in the Hydrostab.

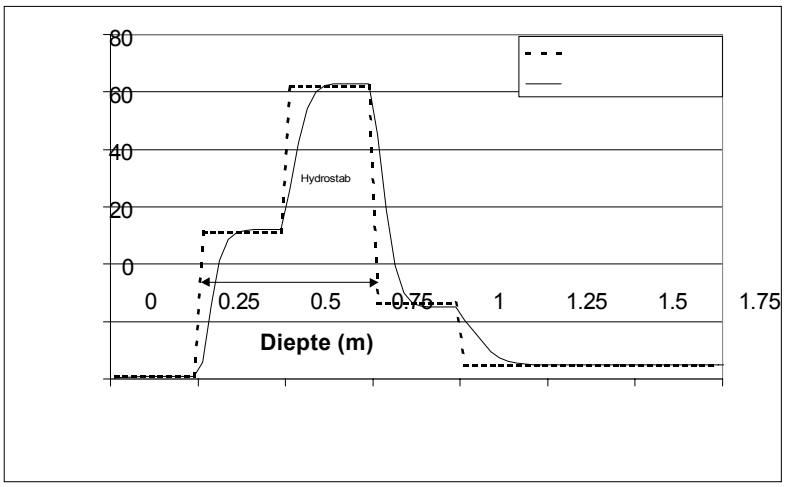

Figure 2 Calculated distribution of the S-concentration and the measured concentration 8years after the construction of the test site. The water flux is less than 1 mm/year

4 Composition and chemical reactions

4.1 Composition of Hydrostab

Hydrostab is an enclosing material developed from residues. The composition and manufacturing of Hydrostab is patented. Hydrostab uses the binding properties of waterglass. The composition of Hydrostab is roughly (Huybrechts en Dijkmans, 2000, Afval Overleg Orgaan, 2002):

1. 40-50 % (polluted) soil or sand (42.5 %)
2. about 10 % flyash (11 %)
3. 40-45 % sewage sludge (42.5 %)
4. 1-5 % waterglass (4 %).

Here the numbers between brackets are from (Afval Overleg Orgaan, 2002).

From a chemical perspective the individual components have their characteristic role in the mixture:

1. Mineral fraction
The soil or sand fraction forms the matrix and is chemically inert .

2. Flyash
Fly ash gives a number of chemically extremely important characteristics to the mixture: Fly ash consists mainly (60-80 %) of amorphous, pozzolan mineral substances of which silicate glasses (am. SiO_2, am. Si-Al-oxides, Calcium-Silicate-glasses) form the main part (Fan et al., 1999, Palomo et al., 1999). Fly ash also contains a lot of iron-oxides and also some free calciumoxide (CaO) . Deze laatste component, evenals de calciumsilicaat-glazen, gaat in contact met water een cementvormende reaktie aan met de (overige) aanwezige pozzolanen lower vorming van C-S-H-gel (Calcium-Silicaat-Hydraat). C-S-H-gel is een hoofdbestanddeel van beton, en geeft mede aan beton haar karakteristieke eigenschappen(lage doorlatendheid, lage porositeit, duurzaamheid). Tenslotte bevat vliegas calciumsulfaat. Dit calciumsulfaat reageert met water lower vorming van gips
(calciumsulfaat-dihydraat). De oplosbaarheid van het gips bepaalt in hoge mate de concentratie calcium in de poriënoplossing.

3. Sewage sludge
Sewage sludge consists of organic colloidal and inorganic substances such as clay minerals and fine silt. These substances increase the plasticity, give a low permeability and increase the water holding capacity (Huybrechts and Dijkmans, 2000).

The pH of sewage sludge is neutral. The buffercapacity is very large, and therefore capable of neutralizing pH effects of the other components. Sewage sludge contains a large pool of exchangeable cations dominated by calcium. When waterglass is added cation exchange will produce a large amount of calcium ions. These ions play a crucial role in the formation of C-S-H gel. Also a reaction occurs between the organic colloids and the silicate colloids of the waterglass, giving extremely stable organic silicate gel structures (Coradin and Lopez, 2003).

4. Waterglass
Waterglass (a solution of sodiumsilicate) reacts with the colloids of the sewage sludge and the Ca-oxides and pozzolan silicate glasses of the fly ash to form (organic) silica gel (SiO2-gel) and C-S-H-gel. These gels block the pore space thus disabling the transport of water.

The result, Hydrostab, is a material with a high waterholding capacity and a very low permeability. The plastic deformability is high, no formation of cracks occurs. Drying out shrinkage sensitivity is low because water cannot evaporate since all pores are blocked. The stability of the Hydrostab depends on the stability of the SiO2 and C-S-H gels: when cristallisation of the gels occurs it will diminish the blocking of the pore space. Then more water flow will occur. Also water evaporation might lead to drying out shrinkage and therefore to the formation of cracks. Finally the plasticity will decrease (the material will become brittle). Drying leads to an irreversible collapse of the gel structure.

The pore water composition of the Hydrostab layers is measured for this project. It is important to keep in mind that the Hydrostab layer has been constructed 8 years ago. The results are given in table 6.

Table 6 Composition of pore water in the Hydrostab layer

Depth cm	code	%Water	pH	Ec mS	Cl ppm	Ca ppm	Na ppm	S ppm	Si ppm
0 - 25	Foot	29.90	7.84	3.46	63.81	472.78	320.10	373.28	245.50
0 - 25	Middle	27.77	7.57	3.83	67.18	405.85	483.35	426.10	260.50
0 - 25	Top	26.98	7.30	6.50	64.16	745.50	823.85	822.19	250.00
25-50	Foot	29.90	7.44	9.72	295.12	901.73	1655.79	1423.14	270.50
25-50	Middle	22.78	7.55	10.70	182.04	1431.76	1376.38	1058.31	269.50
25-50	Top	26.10	7.77	10.09	86.68	743.00	1785.51	1639.83	243.00
0 - 25	Average	28.22	7.57	4.59	65.05	541.38	542.43	540.52	252.00
25-50	Average	26.26	7.59	10.17	187.94	1025.50	1605.90	1373.76	261.00

4.2 The Chemistry of the formation of Hydrostab

When Hydrostab is made, two important gels are formed: Silica-gel and C-S-H-gel. The most important reactions involved are:

4.3 Polymerization of dissolved siliciumdioxide

Mono silicic acid (H_4SiO_4) has at ambient temperatures and in the pH range of 2 - 9.5 a maximal concentration < 100 mg Si/l (100 ppm Si) (Iler, 1979). Above the pH range mentioned the species $H_3SiO_4^-$ en $H_2SiO_4^{2-}$ are important and thus the maximal concentration is higher.

Increase in silicic acid concentration leads to the following nucleophile substitution reaction (SN2):
$H_4SiO_4 + H_4SiO_4 \Leftrightarrow H_6Si_2O_7 + H_2O$ (2 monomers ⇔ 1 dimer)

This leads to a Si-O-Si (siloxane) bound. This polymerization reaction is catalysed by the presence of sufficient $Si\text{-}O^-$ group, i.e. at higher pH values.
Trimers, tetramers and oligomers develop by the same mechanism. The oligomers are mainly condensed, 3-dimensionally linked, not chains. Thus originates a sol of colloidal particles with a diameter of 2-3 nm. Above pH=7 the formation of these colloidal particles is very fast.
Figure 3 (Coradin en Lopez, 2003) schematically shows the process.

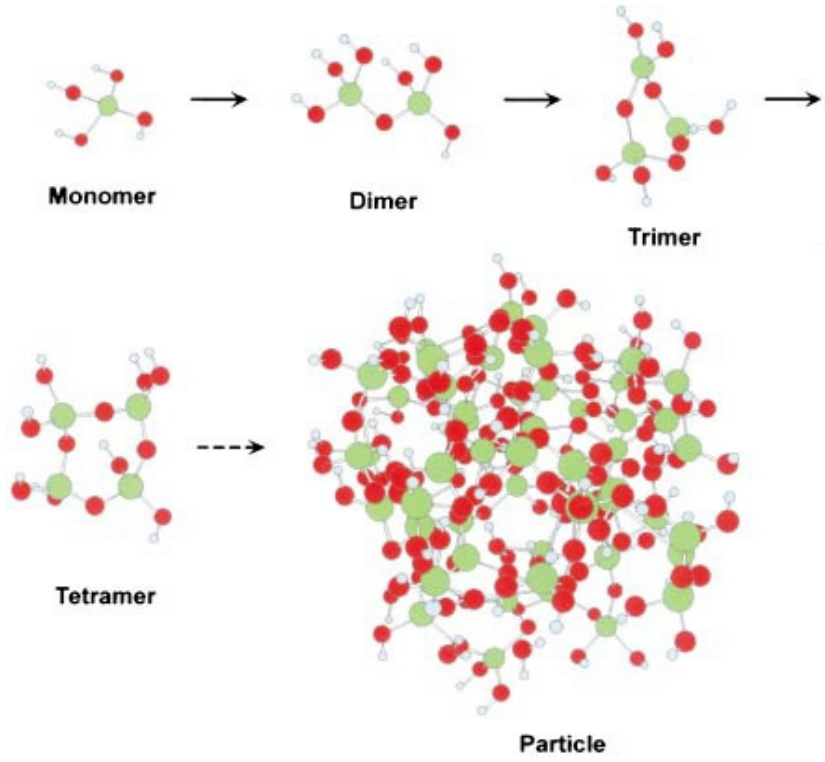

Figure 3 Schematic representation of the formation of polymers from the H_4SiO_4 monomer (Coradin en Lopez, 2003)

The formation of the sol is followed by a process called Ostwald ripening: the solubility of the particles decrease with increasing size. Therefore smaller particles dissolve and precipitate again on the larger particles, until the difference in solubility between the smallest and the largest particles is negligible. Therefore, at pH > 7 and room temperature, and in the absence of cations, a sol with particles of 5-10 nm will develop. Because the surface charge of the particles is negative no further interaction occurs, thus giving a stable *sol*, where the stability increases with increasing pH.

Cations (Na and K, polyvalent cations like Ca and Mg) influence the process: By adsorbing onto the negative surfaces the repelling forces between the particles are neutralized. Thus the particles can approach each other enough to interact and aggregate.
This leads to the formation of a 3-dimensional random, unstructured network of colloidal particles which fill the space, forming a *gel*. This process is called *coagulation*. Also organic cationic poly-electrolytes have the same effect.
With the coagulation the interaction is not restricted to silicate colloids, but also other constituents of Hydrostab participate. In general when hydroxyl groups are available they can interact with the silicate colloids. Examples are the oxides of iron from the fly ash, phenolic and alcoholic groups of the organic matter and clay minerals from the sewage sludge. The reaction is:

$$R\text{-}OH + HO\text{-}Si\text{-}(\ldots.)_n \Leftrightarrow R\text{-}O\text{-}Si\text{-}(\ldots.)_n + H_2O$$

Here R represents the solids (oxides, organic, clay).
The overall effect of this is that the Hydrostab is glued together, all solid particles stick onto each other through silicate-polymers. The final effect is that the pore-space is filled to a large extend with silica-gel, and the pore water is encapsulated in the chaotic gel structure. The volume fraction of pores inside the silica-gel is large, and can measure up to 80 % dependent on the way the gel was formed (Silva and Vasconcelos, 1999).

4.3.1 Interaction between waterglass and fly ash

Fly ash contains a large amount of pozzolan materials (silicate glasses, oxides of aluminum). The pozzolans can be activated (made reactive, hydrated) by conditioning the fly ash with a strongly alkaline solution. Waterglass, an alkaline sodium-silicate solution, is an effective activator (Arjunan, 2001).
The alkaline activation of the fly ash produces a substance that is characterized by a large amount of primary and secondary C-S-H gel (Calcium-Silicate-Hydrate) and C-A-H gel
(Calcium-Aluminate-Hydrate) (Fan et al., 1999, Buchwald et al., 2000, Palomo et al., 1999).
Even if in the Hydrostab the fly ash has not been conditioned, there will still be pozzolan reactions between the fly ash and the waterglass. The effect will however be much slower and possibly not complete. Generally > 50 % of the fly ash is transformed into gels. Together with the silica gel which originates from the

waterglass these gels will determine the chemical and physical properties of the Hydrostab.

4.3.2 Speciation of silicic acid in the soil solution

Silicic acid (H_4SiO_4) is a weak acid. The pKz of the first dissociation is 9.7. This means that for pH values below 9.7 the undissociated species is the most abundant form, and above 9.7, $H_3SiO_4^-$ is the dominant form.
Silicic acid polymerizes: long chains and cyclic structures are formed by condensation reactions under elimination of water molecules:
$H_4SiO_4 + H_4SiO_4 \Leftrightarrow H_6Si_2O_7 + H_2O$ (2 monomers ⇔ 1 dimer)
$H_4SiO_4 + H_6Si_2O_7 \Leftrightarrow H_8Si_3O_{10} + H_2O$ (monomer and dimer ⇔ trimer)
$H_4SiO_4 + H_8Si_3O_{10} \Leftrightarrow H_{10}Si_4O_{13} + H_2O$ (Linear tetramer)
$H_4SiO_4 + H_8Si_3O_{10} \Leftrightarrow H_8Si_4O_{12} + 2H_2O$ (Cyclic tetramer)
Etc.

These processes can go on until the molecules are effectively not in solution anymore, but form a separate phase. A silicate-sol has developed, in which the particles are colloidal. The "real" solubility is dominated by monomers, dimers and tetramers (Tanaka & Takahashi, 1999, 2001, Pereira et al., 1998)

Species which exist in the soil solution are (Tanaka & Takahashi,1999) :
Monomers: H_4SiO_4, $H_3SiO_4^-$, $H_2SiO_4^{2-}$, NaH_3SiO_4, KH_3SiO_4, $CaH_3SiO_4^+$, CaH_2SiO_4
Di-mers: $H_6Si_2O_7$, $H_5Si_2O_7^-$, $H_4Si_2O_7^{2-}$, $NaH_5Si_2O_7$, $CaH_5Si_2O_7^+$, $CaH_4Si_2O_7$
Tetra-mers (cyclic): $H_8Si_4O_{12}$, $H_7Si_4O_{12}^-$, $H_6Si_4O_{12}^{2-}$ etc.

The solubility product of amorphous silica (= silica-gel, also called "Opal-A") at 10 °C, the average temperature of the Hydrostab layer is (Rimstidt en Barnes, 1980):

$SiO_2 - am + H_2O \Leftrightarrow H_4SiO_4$ (aq.) $\log K = -2.85$

This "solubility product" however is a hypothetical value, and depends strongly on admixtures of cations, the extend of ordering in the chaotic gel structure, and the specific surface area of the gel. Beside that the value is strongly temperature dependent. Figure 4 shows the temperature dependency of the solubility of amorphous silica compared with the solubility of quartz (Rimstidt and Cole, 1983)

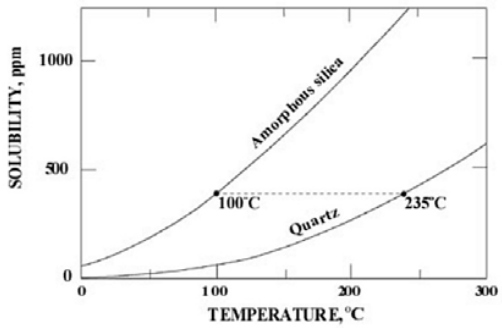

Figure 4 Solubility of quartz and amorphous silica as a function of temperature (Rimstidt and Cole,1983)

Using the speciation, and a chemical equilibrium program, the speciation in the soil solution as a function of the "solubility product" of SiO_2 can be calculated for different pH values. Figure 5 shows the calculated speciation at a pH of 7.5, the pH found in the Hydrostab layers (see table 6).

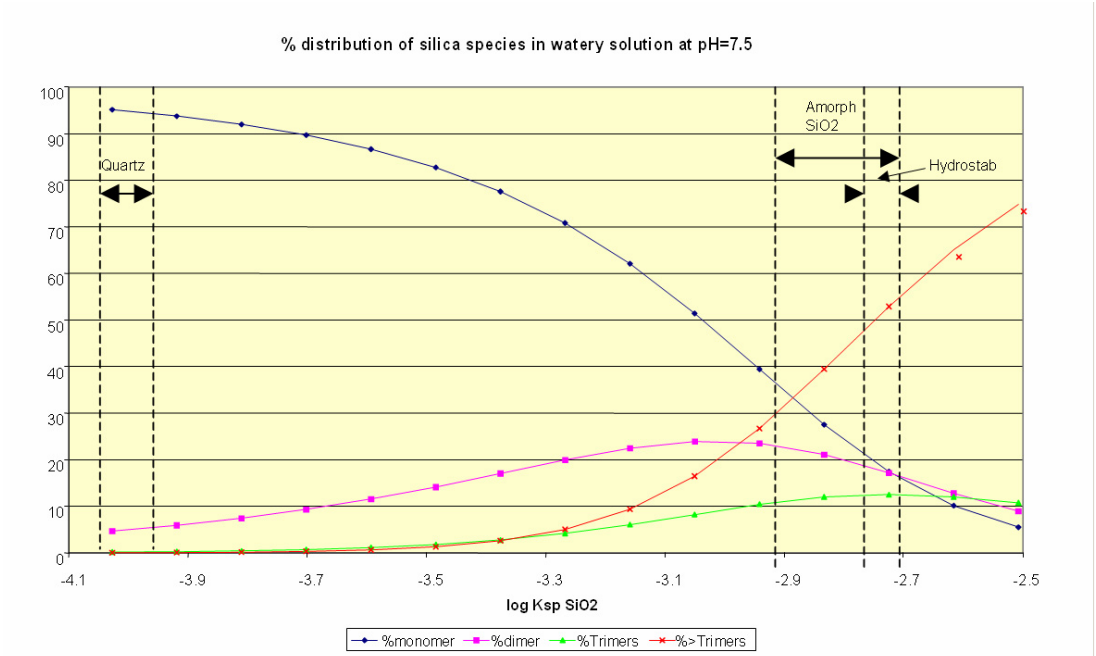

Figure 5 Calculated speciation of the equilibrium solution as function of the solubility product of SiO_2 at pH 7.5 and 10 °C

The result of the calculations show that the speciation of silica in the solution in the Hydrostab layers is dominated by colloids (species > trimers). Monomer silicic acid only forms about 20 % of the concentration in the solution. The solution seems to be supersaturated with respect to amorphous silica (the apparent solubility product is $10^{-2.74}$)
Therefore it looks like silica-gel is still being formed from the solution. This is 8 years after the construction of the Hydrostab layer.

An explanation for this phenomenon is: The C-S-H gel that was formed initially when the Hydrostab layer was constructed, is "undersaturated" and slowly falls apart into calcium ions, hydroxyls and amorphous silica. The hydroxyls react with CO_2 to form bicarbonate ions. This process will continue until all C-S-H gel has been transformed, and up to that time the new formation of silica-gel will continue. Only when the C-S-H gel has disappeared, the crystallization of the silica-gel can start
.

5 Crystallization of Silica-gel

5.1 General Model Structure

5.1.1 Physical Schematization

The model simulates the behavior of Hydrostab in a one-dimensional column of 50 cm length. The column is divided into 10 layers of 5 cm each. The upper boundary value for Si in the pore water is set at 1 mmol Si/l. The model calculates the development of the of the Hydrostab layer for a period of 1000 years with timesteps of 3 months (4 timesteps/year). The temperature of the modelled column within a year is seasonally adjusted: 5 - 10 - 15 - 10 oC.
Results presented are the average values as calculated for the inner 8 layers of the model.

5.2 Mathematical description of the model structure

Units are arbitrary. In principle, it does not matter which units are chosen, as long as the choice is consistent. In this article the following units have been chosen: Amount of the chemical in mol (mol), unit of length in meters (m), surface area in m^2, volume in m^3, and unit of solid mass in kilograms (kg). For any substance in a 1-dimensional column, for a segment i, equation (5.1) applies (Law of mass conservation):

$$(C_i * V_i)_{t+\Delta t} = (C_i * V_i)_t + \Delta t * T + \Delta t * R_i \qquad (5.1)$$

Where
C_i = Concentration of substance in segment i (mol/m^3)
Vi = Volume of segment i, to which Ci applies (e.g. water volume) (m3)
□ t = time step
T = change through transport (mol/time)
R_i = change through reactions occuring in i (mol/time)

Figure 6 gives the general layout for the 1-dimensional transport model.

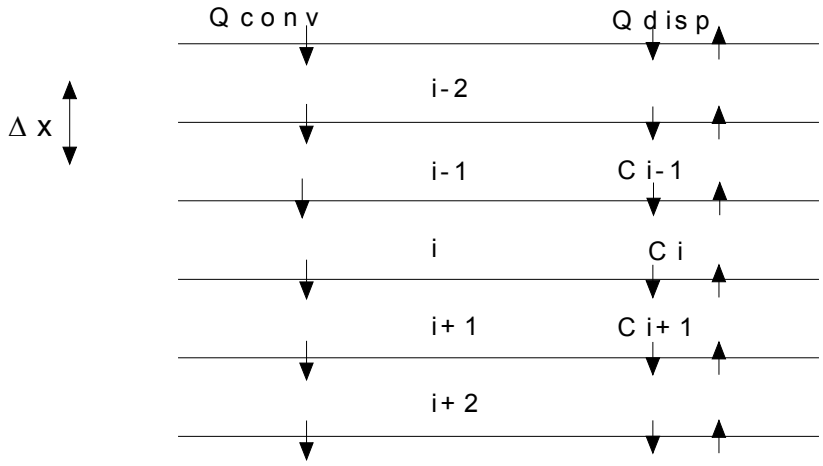

Figure 6 Schemtic drawing of the model of Hydrostab in layers, Δx = 5 cm

The transport term T is made up of two distinct terms: Convection (flow) and diffusion/dispersion (mixing). Focussing on transport through diffusion/dispersion, we can define a mixing volume for the segment interface i-1,i (based on Fick's first law):

$$Q_{i-1,i} = \frac{D_{i-1,i} * SA_{i-1,i}}{0.5*(\Delta x_{i-1} + \Delta x_i)} \qquad (5.2)$$

where
$Q_{i-1,i}$ = mixing volume (m^3/time) for the interface i-1,i
$D_{i-1,i}$ = diffusion/dispersion coefficient for interface i-1,i, with dimension m^2/time (which in itself is a function of tortuosity and/or water fraction, temperature etc.)
$SA_{i-1,i}$= surface area of the interface i-1,i (m^2)
Δx_i = thickness of layer i (m)

Since in this model all segments have the same thickness, $0.5*(x_{i-1} + x_i)$ equals the thickness of the segments, Δx. The surface area of all interfaces in the model is 1 m^2.
The transport through diffusion/dispersion for segment i can be written:

$$T_{dd,i} = Q_{i-1,i} * (C_{i-1} - C_i) + Q_{i,i+1} * (C_{i+1} - C_i) \qquad (5.3)$$

Flow from i-1 to i to i+1 (downward flow) can be brought in (Frissel & Reiniger, 1974): if it is assumed that the concentration which flows from i-1 to i, is the concentration at the interface, this concentration is $(C_{i-1}+C_i)/2$. Similarly, the outflowing concentration is $(C_i+C_{i+1})/2$. If we call the flow rate through the interface $v_{i-1,i}$ resp. $v_{i,i+1}$ and adopt the convention that downward flow (from i-1 to i) is positive (and thus upward flow is negative), then:

$$T_{conv,i} = 0.5 * [v_{i-1,i} * C_{i-1} + (v_{i-1,i} - v_{i,i+1}) * C_i - v_{i,i+1} * C_{i+1}] \quad (5.4)$$

where v = flow in m^3/time.
This discretization of the flow is known in literature as the central-difference scheme, and is the natural outcome of a Taylor-series formulation (Patankar, 1980).

Combining equation (5.1), (5.3) and (5.4) and rearranging the terms for C_{i-1}, C_i and C_{i+1}, gives the mass conservation equation:

$$\begin{aligned} C_{i,t+\Delta t} = \quad & (C_i * V_i)_t / V_{i,t+\Delta t} \\ & + \Delta t * [(Q_{i-1,i} + 0.5 * v_{i-1,i}) / V_{i,t+\Delta t}] && * C_{i-1} \\ & + \Delta t * [-1 * \{Q_{i-1,i} + Q_{i,i+1} + 0.5 * (v_{i,i+1} - v_{i-1,i})\} / V_{i,t+\Delta t}] && * C_i \\ & + \Delta t * [(Q_{i,i+1} - 0.5 * v_{i,i+1}) / V_{i,t+\Delta t}] && * C_{i+1} \\ & + \Delta t * R_i / V_{i,t+\Delta t} && (5.5) \end{aligned}$$

The terms between the square brackets in equation (5.5) form a **tridiagonal** matrix, **A**. In vector notation equation (5.5) can be rewritten as:

$$C_{t+\Delta t} = C_t + \mathbf{A} * C * \Delta t + (R/V) * \Delta t \quad (5.6)$$

where C, R and V are vectors, and **A** is the transport matrix

We define

$$(R/V) = R_0 + R_1 * C \quad (5.7)$$

where R_0 is a vector of zero order rate coefficients ($mol.m^{-3}.time^{-1}$) and
$R_0 \geq 0$ (for stability), and
R_1 is a vector containing first order rate coefficients ($time^{-1}$). Also,

$$C = (1-\vartheta) * C_t + \vartheta * C_{t+\Delta t} \quad (5.8)$$

where $(0 \leq \vartheta \leq 1)$ is the degree of implicitness. The general solution of the set of equations (5.6), (5.7) and (5.8) is:

$$[\mathbf{E} - \vartheta * \Delta t * (\mathbf{A}+\mathbf{E}*R_1)] * C_{t+\Delta t} = [\mathbf{E} + (1-\vartheta) * \Delta t * (\mathbf{A}+\mathbf{E}*R_1)] * C_t + \Delta t * R_0$$

where **E** represents the unity-matrix.

By putting the value of ϑ to 0 we get the so-called *explicit* solution scheme:

$$C_{t+\Delta t} = [\mathbf{E} + \Delta t * (\mathbf{A} + \mathbf{E} * R_1)] * C_t + \Delta t * R_0 \quad (5.10)$$

Examples of explicit models are the soil models of Frissel e.a. (1974), and van Genuchten e.a. (1975). Explicit models have a severe drawback: They are not unconditionally stable. A discussion of stability is given by Press e.a (1986). Generally, explicit models require a time step that assures that the volumes transported are smaller than the segment volumes to remain stable, which make them unpractical to calculate situations with small segment sizes and large transport.

Increasing ϑ increases model stability, with only the value $\vartheta = 1$ assuring unconditional stability without oscillations. The solution scheme is then called *full implicit* and can be found by a matrix-inversion:

$$C_{t+\Delta t} = [\mathbf{E} - \Delta t * (\mathbf{A} + \mathbf{E} * R_1)]^{-1} * (C_t + \Delta t * R_0) \qquad (5.11)$$

This solution scheme is often much more powerful than the explicit scheme because irrespective of the size of the transport terms the solution is stable, and no oscillations can occur. Only when the matrix that has to be inverted is singular then no solution can be found. In practice, this never occurs.

The method described here is based on the work of Crank (1975). Patankar (1980) gives a good discussion of the merits of implicit methods compared to explicit methods. The solution algorithm is also discussed by Press e.a. (1986).

Equation (5.11) is the basic equation of the model presented here.

5.3 Kinetics of silica precipitation and dissolution

Silica gel (in geochemistry often denominated as Opal-A where A equals Amorphous) is a meta-stable phase. Depending on temperature, moisture regime and time silica gel will turn into quartz, the crystalline, stable end member of the SiO_2 mineral group. However, this transition is hampered by sluggish kinetics. As an intermediate phase a micro-crystalline phase appears, which is denominated Opal-CT (CT = Cristoballite-Tridymite) in geochemistry. The proceeding of the crystallisation follows the course:

$$\text{Silica-Sol (solution)} \Rightarrow \text{Silica-Gel} \approx \text{Opal-A} \Rightarrow \text{Opal-CT} \Rightarrow \text{Quartz}$$

The transition of Opal-A to quartz is slow. Temperature is one of the determining factors. The reaction kinetics of the transition of Opal-A through Opal-CT to quartz is studied in geochemistry mainly for hydrothermal systems (e.g. Takeno et al., 2000). For ambient temperature systems (0-30 ^{o}C) no model was found in the available literature.
Therefore here a model which was developed for hydrothermal systems is used to evaluate the behavior at low temperatures. The model presented here has a high degree of similarity with the model presented by Takeno et al. (2000).

The basic equation of the kinetic model is:

$$\partial m H_4SiO_4/\partial t = k_i * A_i * (1 - Q/K_i) / M \quad (5.12)$$

where Q = Ion Activity Product (IAP) of SiO_2 = mH_4SiO_4

m = molality of free silicic acid, t = time, k_i = dissolution rate constant of the i-th silica mineral, A_i = surface area of the i-th silica mineral, M is the mass of the solution, and K_i = the solubility product of the i-th silica mineral.

This kinetical model can be substituted into equation.(5.11) through the R_0 and R_1 terms for segment i:

$$R_{0,i} = k_i * A_i / M_i$$
and
$$R_{1,i} = - k_i * A_i / (M_i * K_i)$$

For quartz the solubility product is (Rimstidt, 1997)

$$\text{Log } K = -0.0254 - 1107.12 / T \quad (5.13)$$

Here T is the absolute temperature in Kelvin.

For Opal-CT the solubility product is (α-cristoballite, Rimstidt and Barnes, 1980)

$$\text{Log } K = -0.0321 - 988.2 / T \quad (5.14)$$

And for amorphous silica (Opal-A) (Rimstidt and Barnes, 1980)

$$\text{Log } K = 0.3380 - 0.0007889 * T - 840.1 / T \quad (5.15)$$

The reaction rate constants are (Rimstidt, 1997)

$$\text{Log k (quartz)} = -0.7324 - 3705.12 / T \quad (5.16)$$

$$\text{Log k (Opal-CT)} = -0.739 - 3586 / T \quad (5.17)$$

$$\text{Log k (am. silica)} = -0.369 - 0.000789 * T - 3438 / T \quad (5.18)$$

Up to this point the model presented here does not differ from the model of Takeno et al. (2000).

The constants in these equations have been investigated further. In 2004 the US Geological Survey published a report with a critical evaluation of reaction rate

constants (Palandri en Kharaka, 2004). Based on that report it can be concluded that for quartz the best available values for the constants are:

$$\text{Log k (quartz)} = -0.75 - 3855 \pm 100 / T \qquad (5.16a)$$

And for amorphous silica:

$$\text{Log k (am. silica)} = -0.475 - 0.000789 * T - 3438 / T \qquad (5.18a)$$

The Hydrostab system contains C-S-H gel. For this gel no kinetic equations have been found in the available literature.
Therefore it is assumed here that the necessary data can be deduced from the Hydrostab solution data as given in table 6. It is however necessary to make some assumptions.
The first assumption that is needed is that the composition of C-S-H gel in the Hydrostab equals the composition of the mineral Tobermorite ($Ca_5Si_6O_{16}(OH)_2$. 8 H_2O, Chen et al., 2002). From the solubility measurements given by Chen et al. (2002) a solubility product can be calculated. It is assumed that the dissolution of C-S-H gel can be modelled with the equation 5.19:

$$\partial H_4SiO_4 / \partial t = k_{C\text{-}S\text{-}H} * A_{C\text{-}S\text{-}H} (1 - IAP/Ksp) / M \qquad (5.19)$$

Using the measurements of table 6 the value of $k_{C\text{-}S\text{-}H}$ can be calculated, assuming that the relations 5.15 and 5.18 describe the behavior of amorphous silica, and other phases have no influence.

The log Ksp calculated from the data of Chen et al. (2002) according to the reaction equation:

$$Ca_5Si_6O_{16}(OH)_2 + 10\ H^+ + 6\ H_2O \Leftrightarrow 5\ Ca^{++} + 6\ H_4SiO_4$$

$$\text{Log Ksp} = \log\{[(Ca^{++})^5 * (H_4SiO_4)^6] / (H^+)^{10}\} = 57.5 \pm 2.5$$

And the log IAP from the measurements of table 6 is 47.5 ± 1.7

This means that the term (1 – IAP/Ksp) of equation 5.19 effectively equals 1 (= $1 - 10^{-10}$), so the maximal dissolution rate. By assuming steady state between the precipitation of amorphous silica and dissolution of C-S-H, and further assuming that
$A_{C\text{-}S\text{-}H} = A_{Opal\text{-}A}$, and T = 283 K we can calculate that log $k_{C\text{-}S\text{-}H}$ = -13.4

5.4 Other model equations

5.4.1 The diffusion equation:

Based on the work of Garboczi and Bentz (1992) an equation developed for the diffusivity of cement based systems is used:

$$D/D_0 = 0.0025 + 0.07 * \phi^2 + H(X) * 1.8 * (\phi - 0.18)^2 \quad (5.20)$$

And
$\phi - 0.18 < 0 \Rightarrow H(X) = 0$
$\phi - 0.18 > 0 \Rightarrow H(X) = 1$

D = Actual diffusion coefficient
D_0 = Diffusion coefficient in water
ϕ = Capilary pore space as fraction of the total volume

The capillary pore space is the totale pore space minus the gel filled pore space. When the capilary pore space reaches a level below 0.18, no continuous pores exist anymore, and the diffusion has to proceed through the pores and canals in the gel-mass. Above 0.18 continuous pores exist, thus ensuring the diffusion acts mainly through these "open water" channels.
The constant of 0.0025 is the recommended value of Garboczi and Bentz (1992) for concrete which has been amended with amorphous silica ("silica fume").

The assumed value of D_0 is $1.9 * 10^{-9}$ m^2/s, which is at the higher side of values given in literature (Bentz et al., 2000).

5.4.2 Specific surface area of the minerale phases

The specific surface area of the individual mineral phases is difficult to define. Based on data of Jennings (2000) for C-S-H and Lenza and Vasconcelos (2001) for silica gel the following values have been used:

Silica gel (Opal-A)	= 500	m^2/g
C-S-H gel	= 500	m^2/g
Opal-CT	= 5	m^2/g
Quartz	= 0.5	m^2/g

5.4.3 The molar gel volume

For C-S-H-gel the gel pore space is 50 % of the volume (Garboczi en Bentz, 1992) and based on data given by Bentz et al. (2000) the molair volume of C-S-H is chosen

as 101.8 cm^3 / mol SiO_2. This value coincides well with the assumption that the C-S-H is chemically characterized as Tobermorite (assuming ρ-Tobermorite to be 2.6)
For amorphous silica a huge number of values can be found in literature. Values range between < 50 % and > 90% . Silva en Vasconcelos (1999) give values between 50 en 90 % (on average 80 %). A measurement of Paulose (2001) gives a gel-porosity of 82 %. Hayrapetyan (2004) gives porosities as function of gel-specific surface area. Using his data it can be calculated that for a specific surface area of 500 m^2/g, the porosity of silica gel which forms in a watery medium is about 73 % . However all work only applies to pure, clean laboratory circumstances. How the real porosity in a system like Hydrostab behaves cannot be deduced from the data. If substantial interbranching with organic matter occurs, the molar weight of the "unit" cannot be given, but is substantially larger than SiO_2 alone. Also, the silica gel is not free of water. A better formula for the inorganic silica-gel is $SiO_2.H_2O$ (mw=78) since there is structural water in the silica-gel. Based on the literature values a gel porosity of 75 % is chosen. A molar volume of 240 cm^3 /mol SiO_2 is used.

5.4.4 The initial composition of the Hydrostab layer

The initial composition assumed for the Hydrostab layer is:

1. 600 g quartz (sand) / kg Hydrostab (60 %)
2. 30 g C-S-H-gel / kg Hydrostab (3 %)
3. 30 g amorphous silica / kg Hydrostab (3 %)
4. 6 g (1 % of quartz) Opal-CT / kg Hydrostab

The value assigned to Opal-CT has arbitrarily been chosen at 1 % of the amount of quartz.
The gel amounts (3 % C-S-H-gel and 3 % silica-gel) are minimal estimates based on the initial 11 % Fly Ash and another 4 % waterglass-solution (30 % SiO_2). According to this assumption "only" < 45 % of the Fly Ash is activated. Literature generally gives > 60% pozzolans in Fly Ash.

5.4.5 The molar gel volume

For C-S-H-gel the gel pore space is 50 % of the volume (Garboczi en Bentz, 1992) and based on data given by Bentz et al. (2000) the molair volume of C-S-H is chosen as 101.8 cm^3 / mol SiO_2. This value coincides well with the assumption that the C-S-H is chemically characterized as Tobermorite (assuming ρ-Tobermorite to be 2.6)
For amorphous silica a huge number of values can be found in literature. Values range between < 50 % and > 90% . Silva en Vasconcelos (1999) give values between 50 en 90 % (on average 80 %). A measurement of Paulose (2001) gives a gel-porosity of 82 %. Hayrapetyan (2004) gives porosities as function of gel-specific surface area. Using his data it can be calculated that for a specific surface area of 500 m^2/g, the porosity of silica gel which forms in a watery medium is about 73 % . However all work only applies to pure, clean laboratory circumstances. How the real porosity in a

system like Hydrostab behaves cannot be deduced from the data. If substantial interbranching with organic matter occurs, the molar weight of the "unit" cannot be given, but is substantially larger than SiO_2 alone. Also, the silica gel is not free of water. A better formula for the inorganic silica-gel is $SiO_2.H_2O$ (mw=78) since there is structural water in the silica-gel. Based on the literature values a gel porosity of 75 % is chosen. A molar volume of 240 cm^3 /mol SiO_2 is used.

5.4.6 The initial composition of the Hydrostab layer

The initial composition assumed for the Hydrostab layer is:

1. 600 g quartz (sand) / kg Hydrostab (60 %)
2. 30 g C-S-H-gel / kg Hydrostab (3 %)
3. 30 g amorphous silica / kg Hydrostab (3 %)
4. 6 g (1 % of quartz) Opal-CT / kg Hydrostab

The value assigned to Opal-CT has arbitrarily been chosen at 1 % of the amount of quartz.
The gel amounts (3 % C-S-H-gel and 3 % silica-gel) are minimal estimates based on the initial 11 % Fly Ash and another 4 % waterglass-solution (30 % SiO_2). According to this assumption "only" < 45 % of the Fly Ash is activated. Literature generally gives > 60% pozzolans in Fly Ash.

6 Calculation of the durability of Hydrostab

6.1 Calculations and Results

The model calculates a total time of 1000 years with timesteps of 3 months. For all timesteps for every layer of 5 cms the changes in C-S-H-gel, Opal-A gel, Opal-CT and the amount of quartz formed are calculated. The changes occur because of chemical reactions as described, and because of mass transport by diffusion. Then the gel-filled pore space is evaluated. By subtracting this from the total porosity the capillary pore space is found. Research of Grattoni et al., 2001 and Garboczi & Bentz, 1992, shows that in cement structures(and thus also Hydrostab) no continuous pores exist (and thus the permeability ~ zero) when the capillary pore space is lower than 0.18-0.20. In that case transport is only possible through the gel pore space. When the capillary pore space rises above 0.20, continous pores are found and not only the permeability increases exponentially, also the diffusivity increases. To make a conservative estimate about when Hydrostab loses its functional characteristics, it is assumed that when the capillary pore space rises above 0.18 this is the case.
The calculations have been performed for two scenarios: Kinetics according to Rimstidt (1997) and kinetics derived from the data of US. Geological Survey (Palandri & Kharaka, 2004) (referred as USG).
Figure 7 (Rimstidt) and 8 (USG) show the calculated development of the silicate gels in Hydrostab in time. From these graphs it's clear that the kinetics of Rimstidt give a faster decrease in amount of gels than the USG scenario.

The results show that as long as C-S-H gel is present, the amount of silica-gel in the pore space increases. The increase in silica-gel is not equal to the decrease of the C-S-H gel because the C-S-H gel also contains calcium and water. The silica-gel however has a higher porosity than the C-S-H gel. Therefore, the capillary porespace decreases as long as C-S-H is transformed into silica-gel. After all the C-S-H gel has disappeared, the amount of silica-gel starts to decrease. The rate of decrease is strongly dependent on the chosen kinetics: Based on the US. Geological Survey data (2004) it can be assumed that the Rimstidt kinetical parameters give a maximal reaction. Therefore for Hydrostab the Rimstidt parameters represent a "worst-case" whereas the USG scenario represents a more realistic scenario.

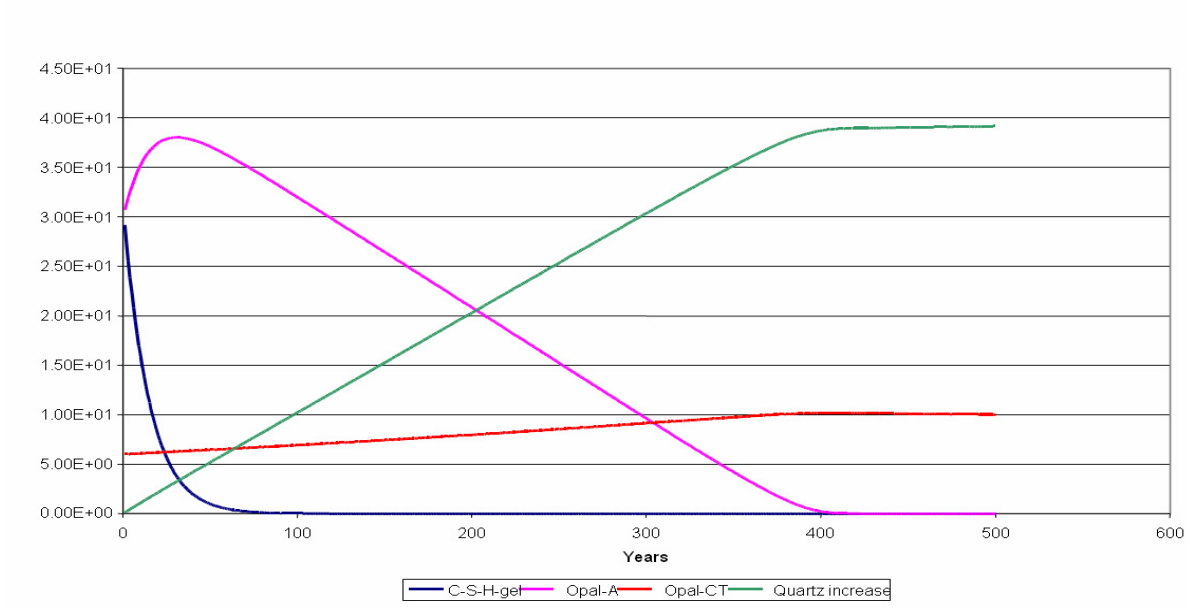

Figure 7 Calculation of the amount of C-S-H-gel, Opal-A, Opal CT and the increase in quartz in Hydrostab (Rimstidt kinetics)

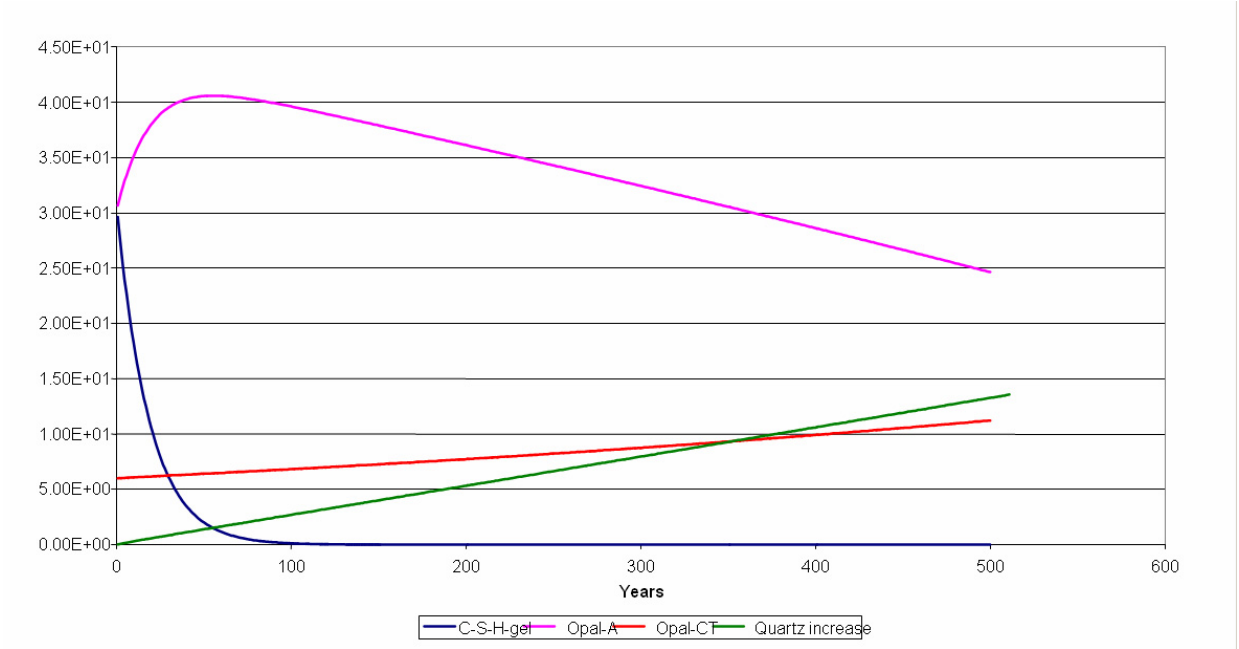

Figure 8 Calculation of the amount of C-S-H-gel, Opal-A, Opal CT and the increase in quartz in Hydrostab (USG kinetics)

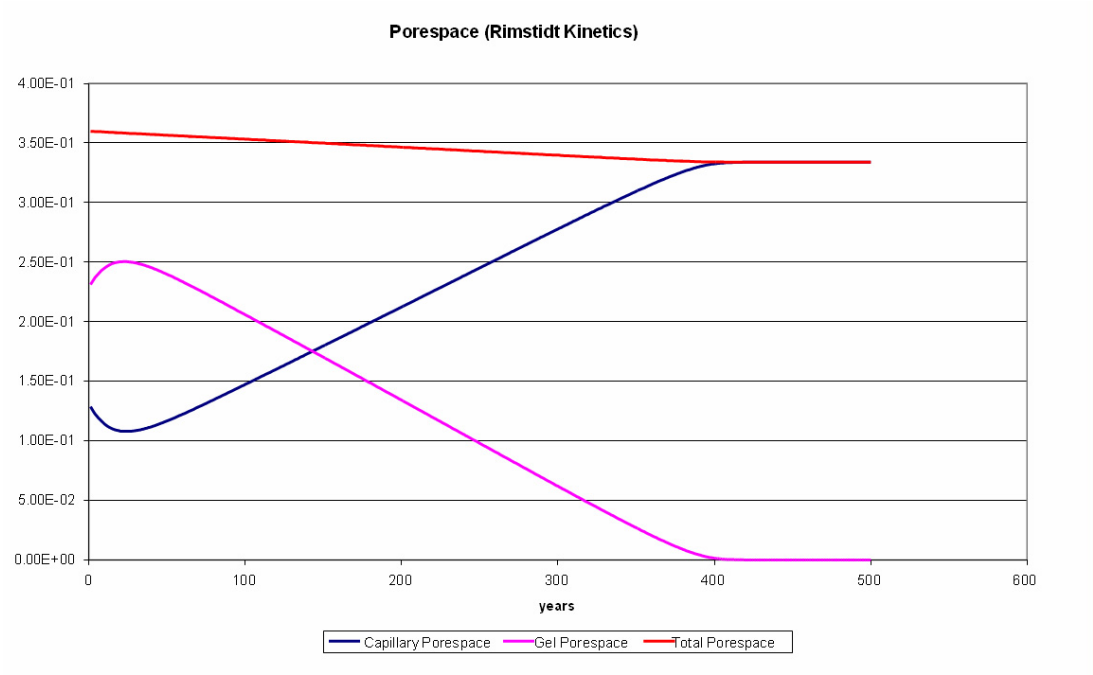

Figure 9 Change of the total pore space, the gel-filled pore space and the capillary pore space calculated with the rates of the Rimstidt scenario.

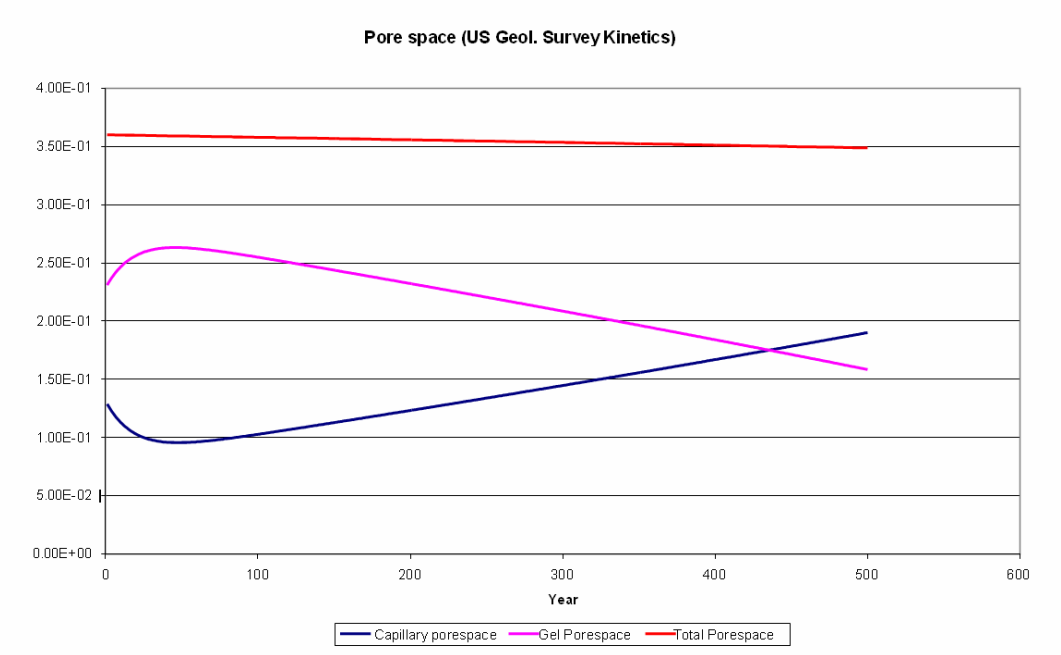

Figure 10 Change of the total pore space, the gel filled pore space and the capillary pore space calculated with the rates of the USG scenario.

Figures 9 (Rimstidt) and 10 (USG) show the development of the pore space in time, distinguishing between total porespace, gel-filled pore space and water filled capillary pores. The decrease in total porosity is caused by the precipitation of quartz and Opal-CT in the capillary pore space. The effect of the different kinetic scenarios is cleary visible.

Finally, figure 11 shows the development of the relative diffusivity (D/D_0) in the Hydrostab layer. It shows that the "critical point" (capillary pore space > 0.18) in the Rimstidt scenario is reached after about 180 years, whereas this point with the USG scenario is only reached after about 500 years.
It follows that the Hydrostab layer, with the given composition, for at least 180 years has such a low diffusivity that mass transport by diffusion is virtually zero.
More likely it takes 500 years before mass transport of any significance takes place.
In the Rimstidt scenario all silicate gels are transformed into christalline compounds in 400 years. Then all that remains is a soil layer with a porosity of 0.34. With the USG scenario, this happens after more than 1000 years.

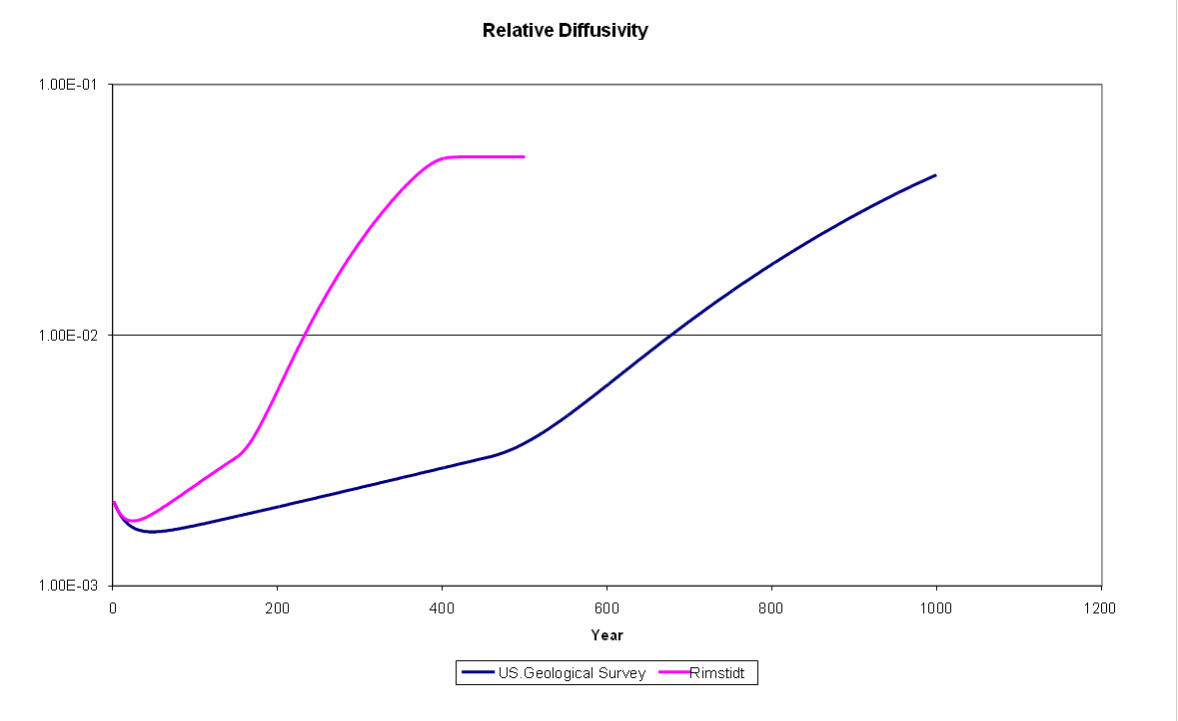

Figure 11 Development of the relative diffusivity (D/D_0) in the Hydrostab layer

6.2 Conclusions

Based on the composition of Hydrostab, and the kinetical modelling of the precipitation/dissolution of the different silicate mineral forms, it can be concluded that Hydrostab is chemically stable for at least 180 years, and upto that point in time will have a permeability that is not significantly different from the initial permeability. It is more likely that it takes 500 years before the Hydrostab becomes less stable.
In the "worst case" scenario the isolating quality of the Hydrostab layer disappears after 400 years. More likely this takes more than 1000 years.

The analysis of the physico-chemical processes shows the importance of the components of the fly ash for the quality and chemical stability of the Hydrostab.
Based on the results of this study it is recommended to investigate the mineral composition of the Hydrostab layer, especially focussed on the appearance and quantity of C-S-H-gel (calcium-silicate-hydrate), and study the composition and pozzolan qualities of the used fly ashes.

Literature

Afval Overleg Orgaan, 2002. Milieueffectrapport Landelijk Afvalbeheerplan, Achtergronddocument A25, Uitwerking "AVI-vliegas". Afval Overleg Orgaan, 2002, pp. 87 (*in Dutch*).

P. Arjunan, M.R. Silsbee, D.M. Roy 2001. Chemical Activation of Low Calcium Fly Ash. I. Identification of suitable activators and their dosage. Proceedings of the Intl. Ash Utilization Symposium, Kentucky, 2001.

D.P. Bentz, O.M. Jensen, A.M. Coats, F.P. Glasser 2000. Influence of Silica Fume on diffusivity in cement-based materials: I: Experimental and computer modeling studies on cement pastes. Cement and Concrete Research, 30 (6), 953-962

Belouschek, P., R. Novotny, 1989. Zur Chemie von pulverförmigen Wasserglas und seinen Folgeprodukten: Kieselsäuresole und -gele in Wasser als Ausgangsmaterial für die Herstellung einer hochwertigen mineralischen Abdichtungsschicht aus bindiger Böden. Müll und Abfall. 12: 636-643 (*in German*)

BKB, 1995a. ‚Toepassing van afvalstoffen in een waterdichte, niet uitlogende, afdeklaag upperop een vuilstort, ter vervanging van de zand-bentoniet en HDPE-folie afdeklaag'. Dalfsen, BKB-Reststoffenmanagement. (*in Dutch*)

BKB, 1995b. ‚Toepassing van afvalstoffen in een waterdichte, niet uitlogende, afdeklaag upperop een vuilstort, ter vervanging van de zand-bentoniet en HDPE-folie afdeklaag; Deelrapport 1'. Dalfsen, BKB-Reststoffen Management. (*in Dutch*)

Boels, D. en J. Beuving, 1996. Afdichtende functie van met waterglas-geïmmobiliseerde afvalstoffen. Wageningen, DLO-Staring Centrum. Rapport 482, 27 blz.; 4 fig.; 3 tab.; 9 ref.; 1 bijl.

Boels, D., 1993. ‚Studie naar lowerafdichtingsconstructies voor afval en reststofbergingen'. Wageningen, DLO-Staring Centrum. Rapport 247.

Boels, D., E.P.W. Koenis en E.M. Loovers, 1993. ‚Geschiktheid van tertiaire kleien en waterglas voor de afdichting van afval- en reststofbergingen'. Wageningen, DLO-Staring Centrum. Rapport 291. (*in Dutch*)

Bril, J., L. Postma, 1993. A management model to assess the extent of movement of chemicals through soils. Proc. 1st Int. Conf. on Delayed Effects of Chemicals in Soils and Sediments, ed. G.R.B. ter Meulen, W.M. Stigliani, W. Salomons, E.M. Bridges and A.C. Imeson, Publ. Stichting Mondiaal Alternatief, Hoofddorp, Netherlands, pp. 181-194

Buchwald, A ., Ch. Kaps, M. Hohmann, 2000. Alkali-Activated binders and pozzolan cement binders - Compete binder reaction or two sides of the same story? http://www.uni-weimar.de/Bauing/bauchemie/Downloads/Bu-Ka-Ho- Manuscript-ICCC.pdf

Chen. J.J., J.J. Thomas, H.F.W. Taylor, H.M. Jennings, 2002. Solubility and structure of Calcium-Silicate-Hydrate. Submitted to: Cement and Concrete Research. http://www.civil.northwestern.edu/people/thomas/pdf/JJTpubs.htm

Coradin, T. and P.J Lopez, 2003. Biogenic Silica Patterning: Simple Chemistry or Subtle Biology? ChemBioChem, 2003, 3, pp 1-9

Crank, J., 1975. The mathematics of diffusion, 2nd edition. Oxford Science Publications, Clarendon Press, Oxford (UK)

Fan, Y., S. Yin, Z. Wen, J. Zhong, 1999. Activation of Fly Ash and its effects on cement properties. Cement and Concrete Research, 29 (4), 467-472

Frissel, M.J. and P. Reiniger, 1974. Simulation of accumulation and leaching in soilsCentre Agric. Publ. and Documentation (PUDOC), Wageningen (the Netherlands)

Garboczi, E.J. and D.P. Bentz, 1992. Computer Simulation of the diffusivity of cement-based materials. Journal of Material Science, 27, 2083-2092 http://ciks.cbt.nist.gov/garbocz/paper24/paper24.html

Grattoni, C. A., A. D. Jing and R.W. Zimmerman, 2001. Disproportionate permeability reduction when Silicat gel is formed in situ to control water production. Argentina, Buenos Aires, SPE Latin American and Carribean Petroleum Engineering Cxonference, 25 – 28 March 2001.

Hayrapetyan, S.S., H.G. Khachatyan, 2004. Problems with the gelling of emulsified colloidal silica. Acta Chromatographica, 14, p. 49-59.

Huybrechts, D. en R. Dijkmans, 2000. Beste Beschikbare Technieken voor de verwerking van RWZI- en gelijkwaardig industrieel afvalwaterzuiveringsslib. Vlaams Kenniscentrum voor Best Beschikbare Technieken (BBT). Vito 2000/IMS/R, rapport 001383, pp. 277. (*in Dutch*)

Iler, R. 1979. The chemistry of silica: Solubility, Polymerization, Colloid and Surface Properties, and Biochemistry. John Wiley and Sons. New York. 866 pp.

Jennings, H.M., 2000. A model for the microstructure of Calcium-Silicate-Hydrate in Cement pastes. Cement and Concrete Research, 30 (1), 102-115

Lenza, R.F.S. and W.L. Vasconcelos, 2001. Preparation of Silica by Sol-Gel Method Using Formaldehyde. Materials Research, 4 (3), p. 189-194

Palandri, J.L., Y.K. Kharaka, 2004. A compilation of rate parameters of water-mineral interaction kinetics for application to geochemical modeling. U.S. Geological Survey Open File Report 2004-1068, pp. 64 http://water.usgs.gov/pubs/of/2004/1068/pdf/OFR_2004_1068.pdf

Palomo A., M.W. Grutzeck, M.T. Blanco, 1999. Alkali-Activated Fly Ashes. A Cement for the Future. Cement and Concrete Research, 29 (8), 1313-1321

Patankar, S.V., 1980. Numerical Heat Transfer and Fluid Flow. Hemisphere Publishing Corp., New York (USA)

Paulose, P.I., Gin Jose, Vinoy Thomas, Gijo Jose, N.V. Unnikrishnan and M.K.R.Warrier, 2002. Spectroscopic studies of Cu2+ ions in sol–gel derived silica matrix. Bull. Mater. Sci., Vol. 25, No. 1, February 2002, pp. 69–74.

Pereira J.C.G., C.R.A Catlow, D.G. Price, 1998. Silica Condensation Reaction: an ab-initio study. Chem. Commun., 1998, 1387-1388

Press, W.H., B.P. Flannery, S.A. Teukolsky & W.T. Vetterling, 1986. Numerical Recipes, The Art of Scientific Computing. Cambridge University Press, Cambridge (UK)

Rimstidt, J.D., 1997. Quartz Solubility at Low Temperatures. Geochim. Cosmochim. Acta, 59 (1), p. 77-85

Rimstidt, J.D., H.L. Barnes, 1980. The kinetics of silica-water reactions. Geochim. Cosmochim. Acta, 44, 1683-1699.

Rimstidt, J.D. and D. R. Cole, 1983. Geothermal mineralization I: The mechanism of formation of the Beowawe, Nevada siliceous sinter deposit. American Journal of Science, 283, 861-875.

Silva, R.F. and W.L.Vasconcelos, 1999. Influence of processing variables on the pore structure of silica gels obtained with tetraethylorthosilicate. Materials Research, 2 (3), p. 197-200

Siedek, H. en J.U. Kügler, 1995. ‚Proefvelden op de stortplaats Twente; Oppervlakte-afdichting op basis van waterglasverrijkte residuenmengsels, met actieve scheurbeveiliging; Grondmechanische aspecten'. Duitsland, Essen, Institut für Umweltforschung Schlieben e.V. Rapport nr. 94.02.14. (*in Dutch*)

Takeno, N., T. Ishido, J.W. Pritchett, 2000. Dissolution, Transport and Precipitation of Silica in Geothermal Systems. Proc. World Geothermal Congress 2000, Kyushu-Tohoku, Japan, p. 2943-2948

Tanaka, M., K. Takahashi, 1999. The Identification of Chemical Species of Silica in Sodium Hydroxide, Potassium Hydroxide and Sodium Chloride Solutions by FAB-MS. Analytical Sciences, 15, 1241-1250

Van Genuchten, M. Th. and P.J. Wierenga, 1975. Simulation of One-Dimensional Solute Transfer in Porous Media. New Mexico State University, Bulletin Office, Las Cruces (NM 88003, USA)

Appendix 1 Pictures of Profiles

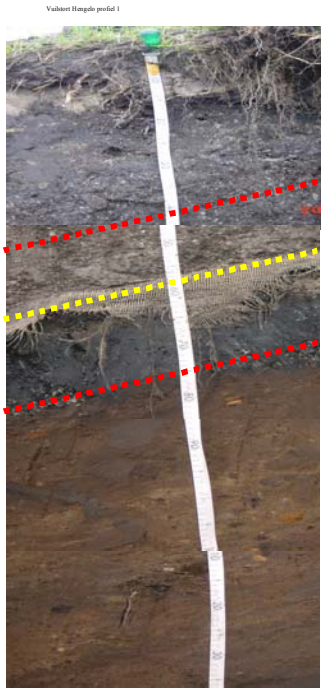

Profile 1 Hengelo Boeldershoek
(Foot of the Middle)

Volume gewicht (kg/m³)	Doorlatendheid (x 10^{-10} m/s) 1996	2004
994	1.4 - 3.0	verstoorde meting
1144		2.22
1124		1.24

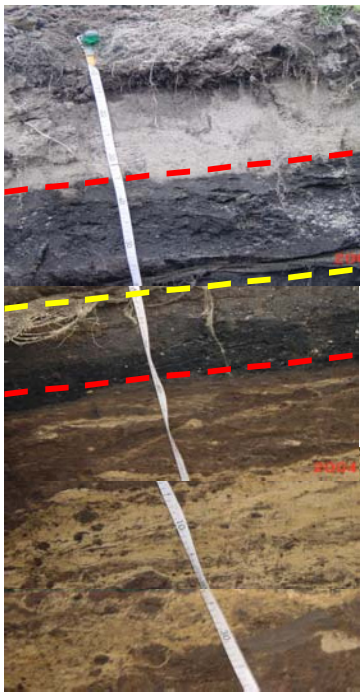

Profile 2 Hengelo Boeldershoek
(middle of the Middle)

Volume gewicht (kg/m³)	Doorlatendheid (x 10^{-10} m/s) 1996	2004
1196	0,7 - 1,4	3,4
1259		gasvorming
1278		1.08

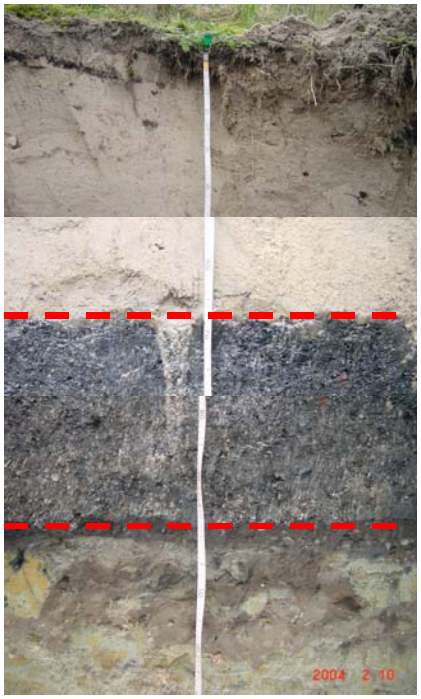

Profile 3 Hengelo Boeldershoek
(top of the Middle)

Volume gewicht (kg/m^3)	Doorlatendheid (x 10^{-10} m/s)	
	1996	2004
1272	3,9 - 6,4	1,74
1185		3,73
1199		1,47

Appendix 2 Profile pits

Profile pit Foot Middle

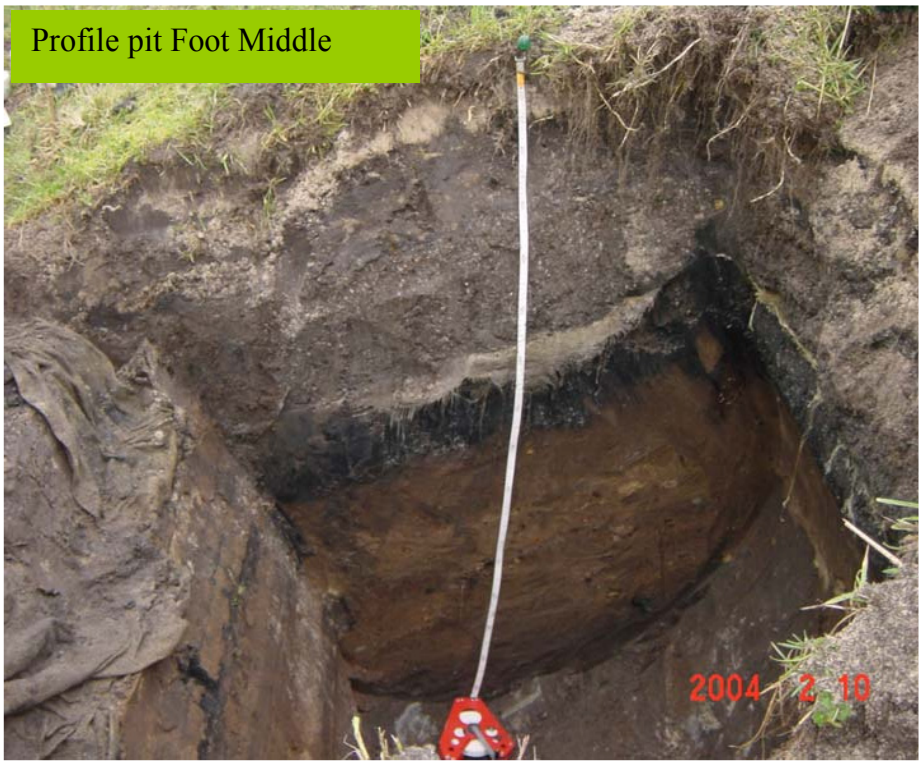

Profile pit middle Middle

Profile pit top of Middle